Short Papers

A New Empirical Large-Signal HEMT Model

Kazuo Shirakawa, Masahiko Shimizu,
Yosihiro Kawasaki, Yoji Ohashi, and Naofumi Okubo

***Abstract*—We propose an empirical large-signal model of high electron mobility transistors (HEMT's). The bias-dependent data of small-signal equivalent circuit elements are obtained from S-parameters measured at various bias settings. And C_{gs}, C_{gd}, g_m, and g_{ds}, are described as functions of V_{gs} and V_{ds}. We included our large-signal model in a commercially available circuit simulator as a user-defined model and designed a 30/60-GHz frequency doubler. The fabricated doubler's characteristics agreed well with the design calculations.**

I. Introduction

Advanced compound semiconductor process technology is making HEMT's common in microwave and millimeter-wave applications. When designing components, accurate large-signal device models are required [1], [2].

In this paper, we propose a new empirical large-signal HEMT model. The bias-dependent data of small-signal equivalent circuit elements are obtained from S-parameters measured at various bias settings [3]. We represented C_{gs}, C_{gd}, g_m, and g_{ds} as functions of V_{gs} and V_{ds}. Considering the charge conservation for C_{gs} and C_{gd}, they were derived from a unique charge source. The drain-to-source characteristics are modeled on the sum of the dc current source and dispersion effect elements.

We characterized an AlGaAs/GaAs HEMT with a gate 0.3 μm long and 100 μm wide in our model, and designed a 30/60-GHz frequency doubler. The fabricated doubler has a conversion loss of 5 dB with a 30-GHz 0-dBm input signal. This data agrees well with the calculations.

II. Large-Signal HEMT Model

To evaluate the large-signal behavior of an HEMT, we first determined the bias-independent extrinsic elements from S-parameters measured up to 62.5 GHz at a typical A-class amplifier's operating bias. And the intrinsic elements are determined as functions of V_{gs} and V_{ds} from S-parameters measured at various bias settings [3]. However, it is desirable to use few equations to represent the large-signal behavior of the device. Considering both accuracy and calculation costs, we chose C_{gs}, C_{gd}, g_m, and g_{ds}, as being bias-dependent. The large-signal HEMT model we proposed is shown in Fig. 1.

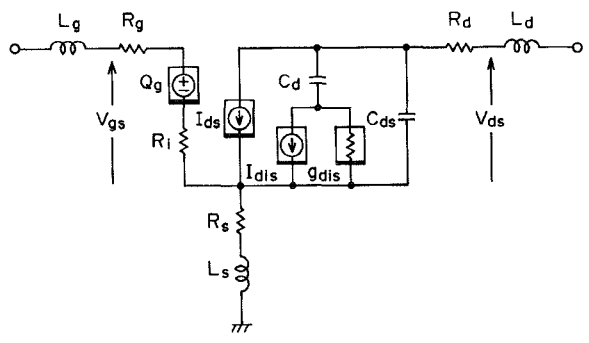

Fig. 1. Large-signal HEMT model.

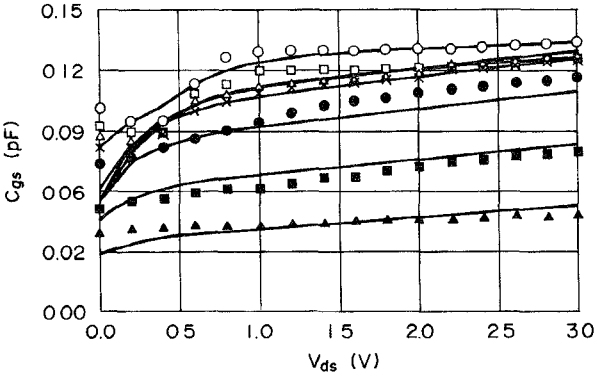

Fig. 2. Large-signal characteristics of C_{gs}. Marks denote data. ○: $V_{gs} = 0.4$ V, □: $V_{gs} = 0.2$ V, △: $V_{gs} = 0.0$ V, ×: $V_{gs} = -0.2$ V, ●: $V_{gs} = -0.4$ V, ■: $V_{gs} = -0.6$ V, ▲: $V_{gs} = -0.8$ V. Solid lines indicate values calculated using our model.

A. Capacitances

Considering the charge conservation for C_{gs} and C_{gd}, the expressions for these capacitances should be derived from a unique charge source. Thus, we assumed this charge source, Q_g, by the following equation.

$$Q_g(V_{gs}, V_{ds}) = Q_0 \frac{\left(\frac{3}{2} + \tan^{-1}(V_J)\right)V_J - \frac{1}{2}\ln(1+V_J^2)}{1+\exp(\delta V_{ds})} \tag{1}$$

where

$$V_J = \gamma(V_{gs} + \alpha\sqrt{V_{gs}^2+1} - V_{ds} + \beta\sqrt{V_{ds}^2+0.1}) \tag{2}$$

is the scaling function, which behaves similar to Staz' function [4]. $Q_0, \delta, \gamma, \alpha$, and β are the fitting parameters. Each parameter in (1) and (2) is obtained by simultaneous curve-fitting for C_{gs} and C_{gd} data.

Fig. 2 compares C_{gs} with the values calculated using (1).

B. Current Source

We assumed the following for a current source. That is

$$I_{ds}(V_{gs}, V_{ds}) = I_0 e^{V_g}[\delta(V_g + V_{g1})V_{ds} + \tanh(\lambda V_{ds})] \tag{3}$$

and

$$V_q = 1 + \alpha\tan^{-1}\beta(V_{gs} + V_{g0}) \tag{4}$$

where $I_0, \delta, V_{g1}, \lambda, \alpha, \beta$, and V_{g0} are the fitting parameters.

These parameters for dc current source, I_{ds}, are obtained by curve-fitting on the dc drain-to-source current. Fig. 3 shows a comparison

Manuscript received June 27, 1994; revised December 18, 1995.

The authors are with Fujitsu Laboratories Ltd., Nakahara-ku, Kawasaki 211, Japan

Publisher Item Identifier S 0018-9480(96)02341-1

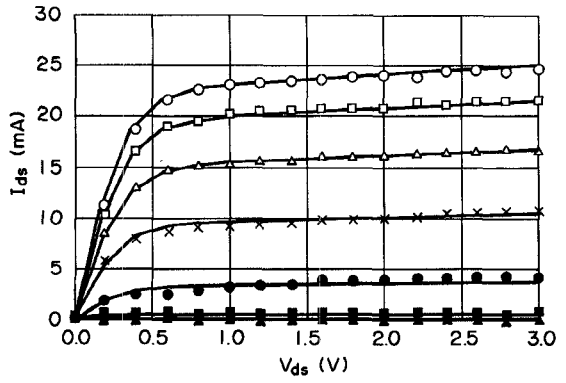

Fig. 3. Dc current characteristics. Marks denote data. o: $V_{gs} = 0.4$ V, □: $V_{gs} = 0.2$ V, △: $V_{gs} = 0.0$ V, ×: $V_{gs} = -0.2$ V, •: $V_{gs} = -0.4$ V, ■: $V_{gs} = -0.6$ V, ▲: $V_{gs} = -0.8$ V Solid lines indicate values calculated using our model.

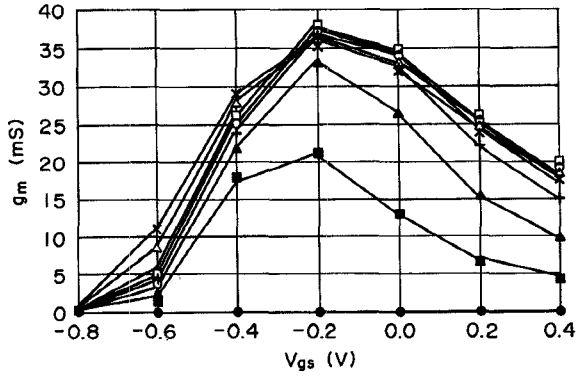

Fig. 4. Large-signal characteristics of g_m. Marks denote data. •: $V_{ds} = 0.0$ V, ■: $V_{ds} = 0.2$ V, +: $V_{ds} = 0.6$ V, o: $V_{ds} = 0.8$ V, □: $V_{ds} = 1.0$ V, △: $V_{ds} = 2.0$ V, ×: $V_{ds} = 3.0$ V Solid lines indicate values calculated using our model.

between this current and the values calculated using the model. There is clearly good agreement.

On the other hand, we modeled the dispersion effect with a capacitance, C_d, conductance, $g_{\rm dis}$, and current source, $I_{\rm dis}$. The current source equation is the same as (3), and $g_{\rm dis}$ is defined as follows.

$$g_{\rm dis}(V_{ds}) = \frac{g_0 V_{ds}}{(1+\alpha V_{ds}^2)} \tag{5}$$

where g_0 and α are the fitting parameters.

For the almost microwave applications, it is adequate to set C_d to several pico-Farads (we set it to 4 pF). Then the fitting parameters in $I_{\rm dis}$ and $g_{\rm dis}$ can be easily determined by comparing the g_m and g_{ds} obtained from S-parameters.

Fig. 4 compares the measured g_m values at RF with values calculated using the equation.

III. 30/60-GHz Frequency Doubler

We included these nonlinear equations in a commercially available circuit simulator as a user-defined model. Table I shows the model parameters for an HEMT with a gate 0.3 μm long and 100 μm wide. The intrinsic elements, R_i, tau, and C_{ds}, are treated as constants fixed at the values corresponding to the particular bias conditions determined by the type of application.

We then designed a 30/60-GHz frequency doubler. Fig. 5 shows the output characteristics of the doubler. It has a 5-dB conversion loss and a 20-dB fundamental signal suppression with a 30-GHz 0-dBm input signal. The operating bias point is $V_{gs} = -0.55$ V, $V_{ds} = 2.0$ V.

In Fig. 5, the crosses denote the experimental data, and the solid lines denote the values obtained by harmonic balance simulation. The model agreed well with the experimental data.

TABLE I
PARAMETERS OF LARGE-SIGNAL HEMT MODEL ($W_g = 100$ μm, $L_g = 0.3$ μm)

Extrinsic Elements

Rg (Ω)	Lg (nH)	Rs (Ω)	Ls (nH)	Rd (Ω)	Ld (nH)
0.016	0.029	0.707	0.004	1.569	0.029

Intrinsic Elements

Capacitances

	Q_0	γ	δ	α	β
Qg	0.350	3.523	-0.078	-1.032	1.009

Drain to Source Characteristics

	I_0	δ	V_{g1}	λ	α	β	V_{g0}
I_{ds}	0.36×10^{-3}	0.43×10^{-3}	5.996	3.268	2.351	4.360	0.533
I_{dis}	1.08×10^{-7}	——		1.912	7.240	3.841	0.736

	g_0	α
g_{dis}	1.11×10^{-3}	0.960

Fixed terms

Ri (Ω)	tau (pS)	Cds (pF)	Cd(pF)
9.50	2.0	0.035	4.0

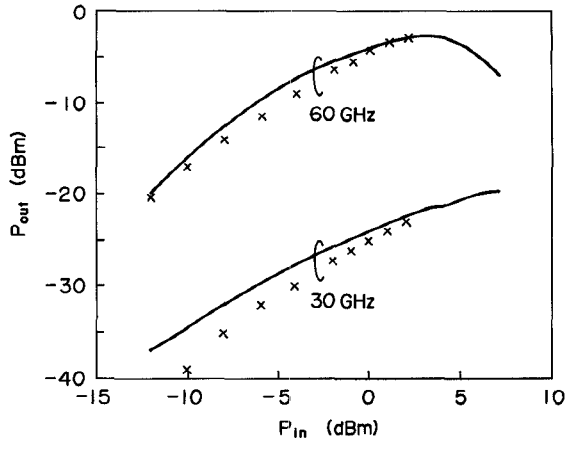

Fig. 5. Input–output characteristics of 30/60-GHz doubler. Bias: $V_{gs} = -0.55$ V, $V_{ds} = 2$ V Crosses indicate measured values and lines indicate values calculated using harmonic balance simulation.

IV. Conclusion

We obtained the bias-dependent data of the intrinsic elements from the S-parameters measured at various bias settings, and made a new

empirical large-signal HEMT model. The principal intrinsic elements, C_{gs}, C_{gd}, g_m, and g_{ds}, are represented as functions of the gate and drain bias voltages.

We characterized an AlGaAs/GaAs HEMT with a gate 0.3 μm long and 100 μm wide with our large-signal model. We included the model in a commercially available circuit simulator as a user-defined element and designed a 30/60-GHz frequency doubler operating at $V_{gs} = -0.55$ V and $V_{ds} = 2.0$ V. The fabricated doubler had a conversion loss of 5 dB with a 30-GHz 0-dBm input signal. The experimental data agreed well with the calculations.

REFERENCES

[1] D. E. Root, S. Fan, and J. Meyer, "Technology independent large signal non quasi static FET models by direct construction from automatically characterized device data," in *Proc. 21st European Microwave Conf.*, Sept. 1991, pp. 927–923.

[2] I. Angelov, H. Zirath, and N. Rorsman, "A new empirical nonlinear model for HEMT and MESFET devices," *IEEE Trans. Microwave Theory Tech.*, vol. 40, pp. 2258–2266, Dec. 1992.

[3] K. Shirakawa, H. Oikawa, T. Shimura, Y. Kawasaki, Y. Ohashi, T. Saito, and Y. Daido, "An approach to determining an equivalent circuit of HEMT's," *IEEE Trans. Microwave Theory Tech.*, vol. 43, pp. 499–503, Mar. 1995

[4] H Staz, P. Newman, I. Smith, R. Pucel, and H. Haus, "GaAs FET device and circuit simulation in SPICE," *IEEE Trans. Electron Dev.* vol. ED-34, pp. 160–169, Feb. 1987.

Efficient Method for Scattering from a Homogeneous, Circular, Cylindrical Shell with an Inhomogeneous Angular-Region

S. Jegannathan

***Abstract*— The two-dimensional (2-D) scalar problem of a circular, dielectric, cylindrical shell exposed to transverse magnetic (TM) incident field is considered. The shell is considered to be homogeneous everywhere, except in a narrow angular-region where it is allowed to be inhomogeneous. The problem is formulated using the moment method (MM). It is shown that the resulting system of MM equations could be very efficiently solved employing a new theory of diagonally-perturbed circulant matrices. The method presented here could be applied for thin shells as well as shells which are "not-so-thin." Results of computer simulations are also provided verifying the validity of the method proposed.**

I. INTRODUCTION

The scattering behavior of various dielectric bodies may be analyzed employing the moment method (MM) [1]. The main limitation of the MM is that it requires the solution of a large, nonsparse system of linear equations. The method demands significant computing resources when implemented directly. It is therefore important to recognize and use any structure present in the coefficient matrix.

In the present work, we consider scattering from a circular, dielectric, cylindrical shell. The shell is considered to be homogeneous everywhere, except in a narrow angular-region where it may be inhomogeneous. We show that the resulting system of MM equations could be efficiently solved employing the new theory of diagonally-perturbed circulant matrices [5] developed in the following sections. An alternative to the approach presented here is to employ the combination of the conjugate-gradient method (CGM) and the FFT [2]–[4]. For the scatterer under consideration, we show that the method presented here works faster than the CGM-FFT technique.

Manuscript received November 16, 1994; revised December 18, 1995.

The author is with the Department of Electrical Engineering, Universiti Malaya, 59100, Kuala Lumpur, Malaysia.

Publisher Item Identifier S 0018-9480(96)02340-X.

II. CIRCULANTS

Consider the $N \times N$ circulant matrix $\mathbf{\Pi}_0$ given by

$$\mathbf{\Pi}_0 = \begin{pmatrix} c_0 & c_{N-1} & c_{N-2} & \cdots & c_1 \\ c_1 & c_0 & c_{N-1} & \cdots & c_2 \\ c_2 & c_1 & c_0 & \cdots & c_3 \\ \vdots & \vdots & \vdots & \ddots & \vdots \\ c_{N-1} & c_{N-2} & c_{N-3} & \cdots & c_0 \end{pmatrix}. \tag{1}$$

The elements of the above matrix may be complex; it is assumed that they satisfy

$$c_r = c_{N-r} \qquad \text{for} \quad r = 1, 2, \cdots, N-1. \tag{2}$$

Let $\mathbf{\Pi}_1, \mathbf{\Pi}_2, \cdots, \mathbf{\Pi}_L$ be matrices such that they are the same as matrix $\mathbf{\Pi}_0$ but with its m_1^{th}, $(m_1, m_2)^{th}$, $\cdots$,$(m_1, m_2, \cdots, m_L)^{th}$, respectively, main diagonal element(s) perturbed by (δ_1), (δ_1, δ_2),$\cdots$, $(\delta_1, \delta_2, \cdots, \delta_L)$, respectively, where m_i, $i = 1, 2, \cdots, L$ are integers such that $1 \le m_1, m_2, \cdots, m_L \le N$, $\delta_1, \delta_2, \cdots, \delta_L$ are arbitrary complex constants; $1 \le L \le N$ and $m_i \ne m_j$ when $i \ne j$. Assuming the appropriate inverses exist, we now have

$$\mathbf{\Pi}_n^{-1} = \mathbf{\Pi}_{n-1}^{-1} - \tilde{\delta_n} \mathbf{v}_{n-1} \mathbf{v}_{n-1}^T \qquad \text{for} \quad n = 1, 2, \cdots, L \tag{3}$$

where

$$\tilde{\delta_n} = \frac{\delta_n}{1 + \delta_n c'_{n-1}}. \tag{4}$$

In the above equations $\mathbf{v}_{n-1}$ and c'_{n-1} are the m_n^{th} column, and the m_n^{th} diagonal element, respectively, of $\mathbf{\Pi}_{n-1}^{-1}$. Equation (3) can be derived as follows: For $n = 1, 2, \cdots, L$, we have

$$\mathbf{\Pi}_n = \mathbf{\Pi}_{n-1} + diag(0 \quad \cdots \quad \delta_n \quad 0 \quad \cdots \quad 0) \tag{5}$$

where in the diagonal matrix of the above equation, δ_n occupies the appropriate m_n^{th} diagonal position. Equation (5) may be written as

$$\mathbf{\Pi}_n = \mathbf{\Pi}_{n-1} + \mathbf{u}_n \mathbf{u}_n^T \tag{6}$$

where $\mathbf{u}_n$ is the $N \times 1$ column vector, all the elements of which are zero except the m_n^{th} element; the m_n^{th} element of $\mathbf{u}_n$ equals $\delta_n^{\frac{1}{2}}$. Now, we have from the matrix inversion lemma [6]

$$\mathbf{\Pi}_n^{-1} = \mathbf{\Pi}_{n-1}^{-1} - \frac{\mathbf{\Pi}_{n-1}^{-1} \mathbf{u}_n \mathbf{u}_n^T \mathbf{\Pi}_{n-1}^{-1}}{1 + \mathbf{u}_n^T \mathbf{\Pi}_{n-1}^{-1} \mathbf{u}_n}. \tag{7}$$

Evidently

$$\mathbf{\Pi}_{n-1}^{-1} \mathbf{u}_n = \sqrt{\delta_n} \mathbf{v}_{n-1}. \tag{8}$$

From (2) and (5), for $n = 1, 2, \cdots, L$ we have

$$\left(\mathbf{\Pi}_{n-1}^{-1}\right)^T = \mathbf{\Pi}_{n-1}^{-1}. \tag{9}$$

Transposing both sides of (8), and substituting (9), we get

$$\mathbf{u}_n^T \mathbf{\Pi}_{n-1}^{-1} = \sqrt{\delta_n} (\mathbf{v}_{n-1})^T \tag{10}$$